Fréedericksz transition in a thermoreversible nematic gel

Matthias Müller,* Wolfgang Schöpf,† and Ingo Rehberg‡
Experimentalphysik V, Universität Bayreuth, D-95440 Bayreuth, Germany

Andreas Timme§ and Günter Lattermann‖
Makromolekulare Chemie I, Universität Bayreuth, D-95440 Bayreuth, Germany
(Received 25 September 2007; published 12 December 2007)

A thermoreversible (physical) gel of a nematic liquid crystal in its planar configuration is investigated. The transition temperatures of the gel are thermally and rheologically determined. The temperature for the nematic-isotropic transition is higher than that for the gel-sol transition, allowing the network to grow in the oriented nematic phase. The electrical Fréedericksz transition of the gel is investigated by using both an optical and an electrical detection method. The transition can be adjusted within a large voltage range by selecting the temperature of the sample. This behavior is determined by the thermal properties of the thermoreversible gel network.

DOI: 10.1103/PhysRevE.76.061701 PACS number(s): 61.30.Gd, 82.70.Gg, 64.70.Md, 83.80.Kn

I. INTRODUCTION

Generally, a simple gel consists of a solid network, which is interspersed (swollen) by a liquid [1]. If a liquid crystal is used as the fluidic component, one obtains liquid crystalline gels with a network, which can either be chemically (irreversibly) or physically (reversibly) cross linked. Because of their combination of mesomorphic and elastic properties, both different kinds of liquid crystalline gels recently gained considerable interest with respect to theoretical [2–9] as well as to application aspects [10–18]. Besides their mechanical behavior, their electro-optical properties have been the focus of these research activities.

The electrically induced Fréedericksz transition [19,20] is the basic working principle of liquid crystal displays. A nematic liquid crystal with a positive dielectric anisotropy $\epsilon_a > 0$ tends to orient parallel to an electric field. When the liquid crystal is placed between two transparent electrodes which have been treated in such a way, that the director $\hat{n}$ is fixed in the plane of the electrodes (planar alignment), and an electric field is applied across the electrodes, the elastic forces counteract this tendency. The voltage, where the electric and the elastic forces are of equal size, is given by the Fréedericksz threshold voltage

$$U_F = \pi \sqrt{\frac{k_{11}}{\epsilon_0 \epsilon_a}}. \tag{1}$$

U_F only depends on the splay elastic constant k_{11} and the dielectric anisotropy ϵ_a. Above threshold, the nematic molecules turn out of the planar alignment and orient, with increasing voltage, more and more parallel to the electric field. For voltages high above threshold, an almost homeotropic configuration results, i.e., the preferred axis is now perpendicular to the electrodes throughout the cell.

Several theoretical analyses of the influence of networks on the electro-optical properties of liquid crystalline elastomers and gels have been presented [2–9]. These systems consider covalently cross-linked polymers swollen by a liquid crystal. Mostly, an increase in the threshold voltage and a decrease in the switching speed toward the planar configuration was predicted. However, the models and results have been quite different, because of different presumptions with respect to structure, deformation and orientation of the network as well as anchoring of the liquid crystal molecules to it.

Contrary to networks built up by covalently cross-linked junction points, physical networks are formed by weaker interaction forces, such as hydrogen bonding. Here, the network disintegrates when heated above a certain temperature T_{gs}, the gel-sol transition, and is reformed when cooled below this temperature. For such thermoreversible liquid crystalline gels, either low molecular weight organic compounds [12,13,17,18] or liquid crystalline block copolymers [16] have been used as appropriate gelators. With respect to these gels, experimental investigations on the switching behavior in twisted or super-twisted nematic display configurations have already been described in the literature [11,14,15].

The present paper deals with a nematic liquid crystalline mixture as the liquid component of a physical gel with a low molecular weight organogelator in a very low concentration (0.2% [21]). We investigate the viscoelastic properties of this gel and their dependencies on the temperature. The materials have been chosen such, that the temperature for the gel-sol transition, T_{gs}, is below that for the nematic-isotropic transition, T_{ni}. Thus, when cooling from the liquid state, the gelation occurs in the nematic phase, which is oriented in a conventional electro-optical cell provided with an orientation layer.

In Sec. II, we describe the preparation of the sample with the thermoreversible nematic gel. Thermal and rheological properties of the gel are discussed in Sec. III. In Sec. IV, we study the Fréedericksz transition by applying a birefringence

*matthias.mueller1@uni-bayreuth.de
†wolfgang.schoepf@uni-bayreuth.de
‡ingo.rehberg@uni-bayreuth.de
§andreas.timme@uni-bayreuth.de
‖guenter.lattermann@uni-bayreuth.de

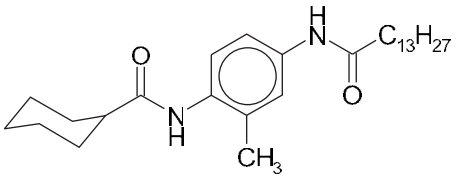

FIG. 1. Gelator: *N*-(2-methyl-4-tetradecoylamino-phenyl)-cyclohexanecarboxamide.

method and by measuring the complex conductivities of the samples. Finally, in Sec. V, we summarize our findings.

II. SAMPLE PREPARATION

We use the liquid crystalline mixture E49, obtained from Merck [22]. It consists of cyanobiphenyls and cyanoterphenyls, substituted in the paraposition with aliphatic chains of different length [23]. E49 is nematic at room temperature and shows the nematic-isotropic transition at a clearing range of $T_{ni}=102\ ^\circ\mathrm{C},\ldots,112\ ^\circ\mathrm{C}$ in polarizing microscopy. From our measurements, we find a positive dielectric anisotropy of $\epsilon_a \approx 15$ and a threshold voltage $U_F^{\mathrm{E49}}=0.88$ V for the Fréedericksz transition. Unfortunately, no material parameters are supplied by Merck.

The gelator *N*-(2-methyl-4-tetradecoylamino-phenyl)-cyclohexanecarboxamide (see Fig. 1) has previously been synthesized [24]. This low molecular weight organogelator can gelify liquid crystals at very low concentrations. The gelator molecules self-assemble through intermolecular hydrogen bonding, building up rodlike or fiberlike crystalline structures that interweave to form a homogeneous, thermoreversible physical network. The gel becomes liquid above a temperature of around $T=58\ ^\circ\mathrm{C},\ldots,71\ ^\circ\mathrm{C}$ (see Sec. III).

The gel network can be observed by means of scanning electron microscopy (SEM, see Fig. 2). As it is not possible with SEM to investigate gels containing a solvent, i.e., the gels *in-situ*, the liquid crystal E49 has been extracted from the gel, using the very gentle technique with supercritical CO_2 [25]. Unlike with an organic solvent, the extraction in the supercritical state prevents the gel network structure from collapsing so that the pure gel network with the main characteristics of the *in-situ* state remains. This is due to the nonexisting solid-liquid surface tension in a supercritical fluid. The dried xerogel can then easily be investigated by the classical SEM method (Fig. 2). These measurements are performed on a LEO 1530 FE-SEM with a field emission cathode and an Inlens detector.

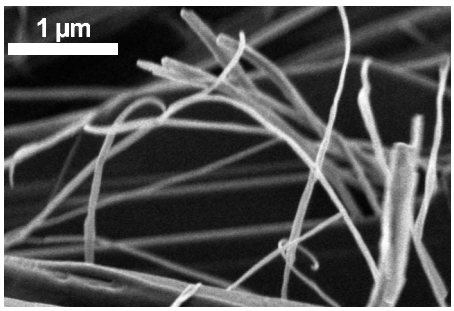

FIG. 2. SEM image of the fiberlike structure of the gel network taken from a xerogel with 0.2% gelator.

The nematic liquid crystalline physical gel itself is prepared by mixing E49 and the gelator in a closed vial, using a concentration of 0.2% of the gelator. The vial is heated to a temperature of 120 °C and kept at this temperature until the gelator has been fully dissolved into the isotropic liquid crystal. The solution is then cooled to room temperature.

For the measurements of the Fréedericksz transition, the typical experimental setup is used, as described, e.g., in Ref. [26]. The samples are prepared in commercially available cells [27]. They consist of two parallel glass plates, which are separated by spacers and which have an indium tin oxide (ITO) layer on the inside. The ITO surfaces of the electrodes are coated with a polymer and rubbed in one direction in order to produce the planar alignment of the liquid crystalline material: when the cell is filled with a nematic material, the director is aligned along the rub direction in the layer plane. The thickness of the cell $d=(25\pm1)\ \mu$m is determined by the spacers between the glass plates.

The empty cell and the vial with the gel are heated to a temperature of $T=130\ ^\circ\mathrm{C}$, where the cell is filled by capillary action. This is well above the gel-sol transition and above the nematic-isotropic transition. In order to remove flow-induced defects which may have formed during filling, the system is kept at this temperature for another 10 min. Finally, it is cooled to $T=10\ ^\circ\mathrm{C}$ within 6 min by a quenching procedure which is similar to the cooling characteristics of the rheometer used for the characterization of the liquid crystalline gel (see Sec. III D). This step is necessary to obtain a super-finely dispersed gelator network structure with minimal disturbances of the director alignment of the liquid crystal. Slower cooling rates lead to the formation of larger dendritic structures caused by the disorientation of the director field through network fibrils. As these dendritic structures considerably disturb the optical investigations, they should be avoided.

III. THERMAL AND RHEOLOGICAL INVESTIGATIONS

The thermoreversible network disintegrates when heated above a critical temperature T_{gs}. There are several methods to characterize this transition.

A. Falling ball method

A simple technique to observe the gel softening on heating is the falling ball method (see, e.g., Ref. [28]). A gel with a volume of 0.2 cm^3 is prepared in a test tube with a diameter of 8 mm. A steel ball (diameter 3 mm, mass 0.11 g) is placed on top of the gel before the test tube is heated with 1 K/min in an oil bath. At a certain temperature, here at $T=56\ ^\circ\mathrm{C}$, the ball sinks inside the gel until it touches the bottom of the test tube. At this temperature, the gel becomes so soft, that it is no longer able to carry the weight of the ball, therefore it is taken as the softening temperature of the gel. The full disintegration of the network, however, occurs at a higher temperature.

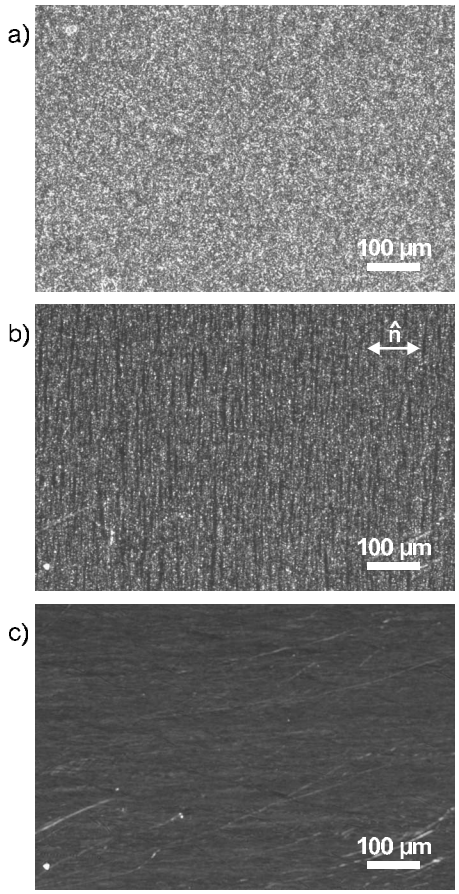

FIG. 3. Polarization microscopy images showing the disappearance of the defect textures: (a) $T=20$ °C, (b) $T=60$ °C, and (c) $T=70$ °C. The preferred direction of the director $\hat{n}$ induced by the orientation layer is indicated by the arrow.

B. Polarizing microscopy

Another possibility to observe the gel-sol transition process is by polarizing microscopy. A sample prepared in a cell as described in Sec. II is investigated between crossed polarizers on an Olympus microscope BX41. The orientation layer of the cell is arranged parallel to one of the polarizers. In this geometry, a planarly oriented liquid crystal would appear dark. If the director alignment of the liquid crystal is slightly disturbed by the network structure, small optical defects can be observed [see Fig. 3(a)]. When heating within a temperature-controlled box, these defects start to disappear at $T=58$ °C and are completely invisible at $T=69$ °C, indicating the disintegration of the network fibers [see Fig. 3(c)].

An interesting feature, namely that these optical defects can be oriented perpendicular to the director $\hat{n}$ [see Fig. 3(b)], indicates that the super-finely dispersed gelator network might be oriented in the same direction. Similar to the phenomenon described by Kato *et al.* [29], the gelator molecules themselves are expected to orient with their long axes parallel to the director of the liquid crystal. They aggregate, however, perpendicular to their long axes and in consequence perpendicular to the director. In our case, this is not achieved by π-π interactions but rather by hydrogen bonding.

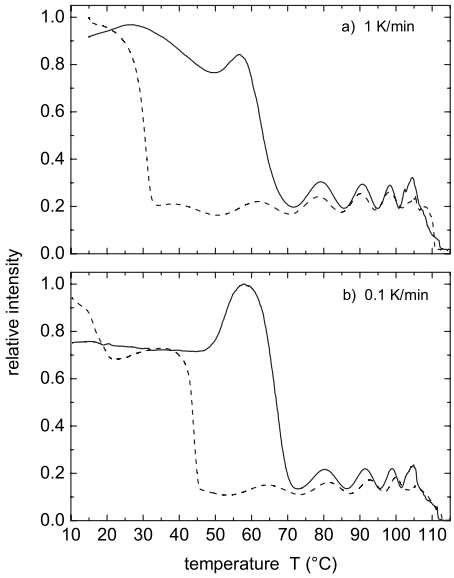

FIG. 4. Transmitted light intensity during melting and reforming of the gel. The solid lines represent the heating processes, while the dashed lines are taken when cooling. The measurements are performed with heating and cooling rates of 1 K/min (a) and of 0.1 K/min (b).

In order to characterize the disappearing of the network in a more quantitative way, we measure the intensity of the transmitted light through the filled cell, using the setup described in Sec. IV A. Two sets of measurements are shown in Fig. 4, which are performed with heating and cooling rates of 1 K/min and 0.1 K/min, respectively. With both heating rates, the intensity starts to decrease at $T=58$ °C and reaches its minimum at $T=71$ °C. As expected, the temperature of the total disintegration of the network is higher than the softening temperature determined by the falling ball method. The reforming of the network on cooling depends strongly on the cooling rate and begins at a temperature of $T=33$ °C in the case of cooling with 1 K/min and at $T=45$ °C when cooling with 0.1 K/min. Since our sample is not perfectly aligned parallel to the polarizer, the signal is superimposed by an oscillation [30], which vanishes when the sample becomes isotropic. This happens in a temperature range of $T_{ni}=102$ °C, … , 112 °C, which is the same as in the case of the pure liquid crystalline mixture.

C. Differential scanning calorimetry

Neither investigations with the standard differential scanning calorimetry (DSC) technique (Diamond DSC, Perkin-Elmer) nor the much more sensitive Micro DSC (Micro DSC III, Setaram) have been successful to detect the gel-sol transition at the given gelator concentration of 0.2%.

D. Rheological measurements

In order to obtain more detailed information about the temperature-dependent viscoelastic properties, rheological measurements are performed, using an Anton-Paar MCR301

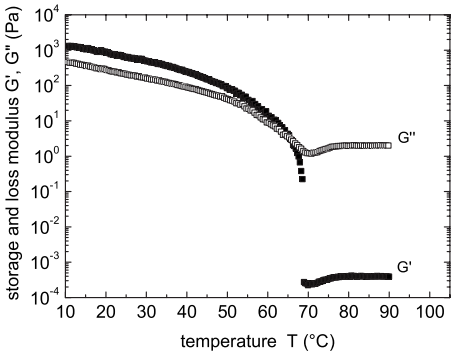

FIG. 5. Rheological properties of the nematic gel as a function of the sample temperature: storage modulus G' (■) and loss modulus G'' (□).

rheometer. The measurement system is a cone-plate geometry with a diameter of 50 mm and an angle of 1°. The temperature is adjusted by Peltier devices in the plate and in a heating mantle placed over the cone. For loading a sample, the plate is heated to $T=90$ °C. The gel is put onto the plate, where it becomes liquid, and the cone is lowered to the measurement position [31]. The measurement starts with a cooling procedure from $T=90$ °C to $T=10$ °C within 6 min, which is the fastest cooling rate possible in this system. The sample is kept at this temperature for 1 hour before it is heated with 1 K/min. During heating, the values of the storage modulus G' and the loss modulus G'' are determined in oscillation mode with a frequency of $f=10$ Hz and a deformation of $\gamma=0.1\%$. For lower oscillation frequencies, the measured torque is below the specified sensitivity of the instrument, whereas higher frequencies lead to a bad ratio of the measurement system's acceleration torque to the sample's torque. The deformation of $\gamma=0.1\%$ is sufficiently low for the sample to remain in the linear viscoelastic regime.

Figure 5 shows G' and G'' as functions of the temperature for such a heating procedure. At low temperatures, the G' curve lies above the G'' curve, i.e., the elastic properties predominate the viscous properties as expected in the gel state. With increasing temperature, G' and G'' decrease. The two curves intersect at $T=66$ °C. The end set of G' is reached for $T=69$ °C, indicating that the elastic properties have disappeared, i.e., the gel network is completely disintegrated as expected in the sol state.

The results depend on the chosen frequency f of the experiment. To determine the gel point, however, one needs a frequency-independent criterion. According to Ref. [32], the gel point T_{gs} is defined as that temperature where the loss tangent $\tan\delta=G''/G'$ becomes frequency independent. To find this temperature, several frequency sweeps of $\tan\delta$ are performed for different temperatures (see Fig. 6). The frequency range is given by the broad gel-sol transition region. A linear regression line is fitted to each data set. Figure 7 shows the slope m of these lines as a function of the temperature, where a slope of $m=0$ indicates frequency independence. Although the theory of Ref. [32] has been developed for chemical gels with a sharp sol-gel transition, in our case of a broad transition, $\tan\delta$ is also almost frequency independent for temperatures of $T\leq 66$ °C. For higher temperatures,

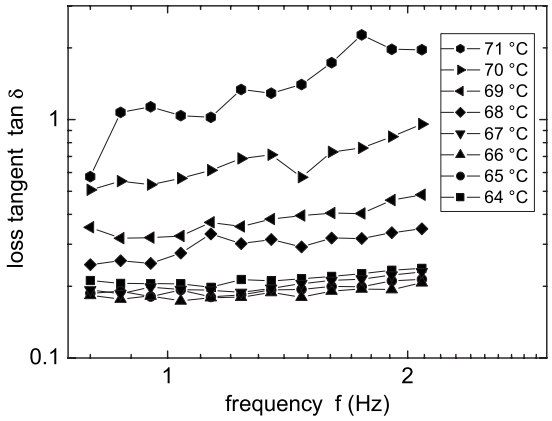

FIG. 6. Loss tangent of the nematic gel as a function of the frequency for several temperatures.

$\tan\delta$ increases with the frequency, so that $T=66$ °C is considered to be the gel-sol transition temperature T_{gs}.

To summarize the results of the various methods, the liquid crystalline gel of 0.2% of our gelator with the liquid crystalline mixture E49 exhibits a gel-sol transition range from $T=58$ °C, ..., 71 °C, with a rheological determined transition temperature $T_{gs}=66$ °C.

IV. ELECTRO-OPTICAL MEASUREMENTS: THE FRÉEDERICKSZ EFFECT

A. Experimental procedure

For measuring the Fréedericksz threshold, we use the samples prepared between two glass plates, as described in Sec. II. A sinusoidal ac voltage with a frequency of 1 kHz is applied across the electrodes by means of a wave-form generator (Agilent Technologies 33220A). The cell is illuminated by a light emitting diode (Luxeon Star LXHL-MD1C) with a dominant wavelength of $\lambda\approx 625$ nm and a spectral bandwidth of $\Delta\lambda=20$ nm. The temperature of the sample holder can be varied from 10 °C to 150 °C with a long-term stability of ±0.2 K. The samples are observed with a polarizing transmission microscope (Olympus BX41) and recorded with a CCD camera (Lumenera Corporation LU135M-IO), that is connected to a computer. The images

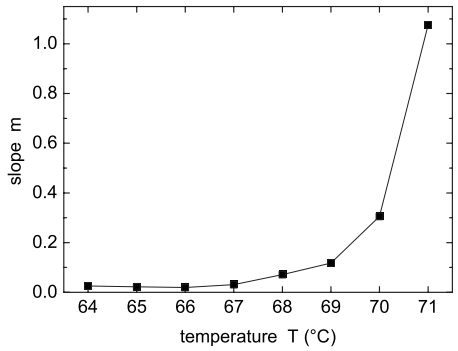

FIG. 7. Slope m obtained from the data depicted in Fig. 6 as a function of the temperature.

have a physical size of 1.20×0.96 mm^2 and a resolution of 1280×1024 pixels.

In order to detect the Fréedericksz transition, we use the birefringence method as explained in Refs. [33,34]. The cell is illuminated with linearly polarized light. By choosing a polarizing angle of 45° relative to the director, the ordinary ray (light polarized perpendicular to the director) and the extraordinary ray (light polarized parallel to the director) have the same intensities. After passing the sample, the two rays interfere in an analyzer perpendicular to the polarizer. When the director starts to turn from the planar to the homeotropic configuration, the length of the optical path of the extraordinary ray decreases. This leads to an oscillation of the transmitted light intensity since constructive and destructive interference of the two rays alternate while the director turns [35,36]. In the limiting case of high voltages, when the director alignment is nearly homeotropic and the optical path lengths become equal for the two rays, the intensity decays to zero [37]. We measure the transmitted light intensity by integrating over the center 256×256 pixels (0.24×0.24 mm^2) of the image taken by the CCD camera.

In addition, we use a lock-in technique as described, e.g., in Ref. [38] to measure the complex conductivity

$$\tilde{G} = \frac{\tilde{I}}{\tilde{U}} \tag{2}$$

of the samples. Here, $\tilde{U} = U_0 e^{i\omega t}$ is the complex voltage and $\tilde{I} = I_0 e^{i\varphi} e^{i\omega t}$ is the complex current with a phase shift φ with respect to the voltage. Current and voltage at the cell are measured at a rate of 500 samples per cycle and averaged over 100 cycles of the applied voltage by means of an AD converter (Data Translation DT9834). From the complex conductivity determined in this way, we calculate the ohmic resistance R and the electric capacity C of the samples,

$$R = \frac{1}{\mathrm{Re}(\tilde{G})} \quad \text{and} \quad C = \frac{\mathrm{Im}(\tilde{G})}{\omega}. \tag{3}$$

The effective ohmic conductivity σ and the effective electrical permittivity ϵ are given by

$$\sigma = \frac{d}{RA} \quad \text{and} \quad \epsilon = \frac{Cd}{\epsilon_0 A}. \tag{4}$$

A is the area of the electrodes and d is the sample thickness. Due to the anisotropy of the material parameters, this method does not yield the local values of σ and ϵ, which, in the case of the Fréedericksz instability, vary inside the cell with the variation of the director [20,38]. Instead, we obtain values which are averaged over the whole active sample volume of $1\ \mathrm{cm} \times 1\ \mathrm{cm} \times 25\ \mu\mathrm{m}$. They are determined by $\sigma_\perp$ and $\sigma_\parallel$, the conductivities perpendicular and parallel to the director, as well as $\epsilon_\perp$ and $\epsilon_\parallel$, the permittivities perpendicular and parallel to the director. In the ground state, when the applied voltage is below the Fréedericksz threshold, the effective values σ_g and ϵ_g are approximately given by $\sigma_\perp$ and $\epsilon_\perp$, respectively, due to the planar alignment everywhere in the sample. They are not exactly equal because of unavoidable director inhomogeneities and, in the case of the gel, because of disturbances by the gel network. For very high voltages, when the alignment is almost homeotropic, σ and ϵ are close to $\sigma_\parallel$ and $\epsilon_\parallel$, respectively. In between these extreme cases, the effective values follow a monotonous function (for details see Ref. [38]).

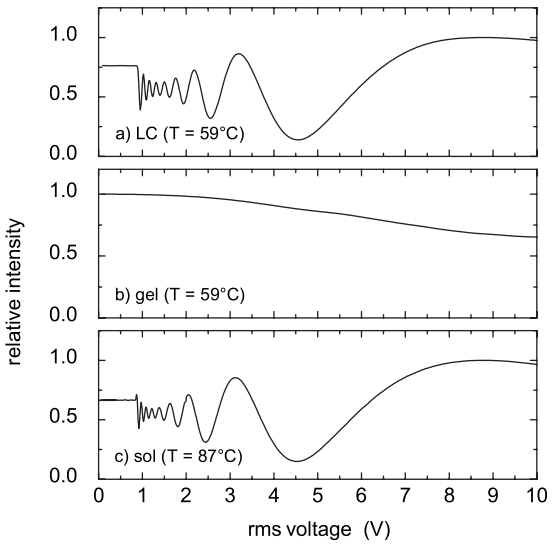

FIG. 8. Optical detection of the Fréedericksz threshold: Transmitted light intensity with crossed polarizer optics as a function of the driving voltage for the pure liquid crystal (a), and for the liquid crystalline gel with (b) an established (gel phase) and (c) a melted (sol phase) gel network.

B. Measurements

We measured the dependence of the Fréedericksz threshold voltage on the sample temperature for our liquid crystalline gel and, as a comparison, for the pure liquid crystal E49. For the gel, the temperature was increased from 15 °C to 40 °C in steps of 5 K and then from 40 °C to 98 °C in steps of 2 K. For the reference measurements with the pure liquid crystal, steps of 5 K were used over the whole range, as there is no significant temperature dependence of the threshold voltage. After each change in temperature, we waited for 3 h before the actual measurement took place. For each temperature, we varied the applied voltage in the range of 0.1 V to 10 V in steps of 25 mV. After a waiting period of 10 s at every step, an image of the sample was taken and the complex conductivity was measured, as described in Sec. IV A.

As is typical for the Fréedericksz transition, and has been explained in Sec. IV A, the intensity of the light transmitted through the pure liquid crystal shows oscillations as a function of the applied voltage above the Fréedericksz threshold [Fig. 8(a)]. The intensity would decrease to zero for higher voltages. In contrast, the behavior for the gelified sample is quite different [Fig. 8(b)]. Here, the main effect is a decrease in the transmitted light intensity. This decrease starts at a higher voltage than for the pure material, and due to the distortion of the director field caused by the network structure, there is no longer a sharp onset visible. At higher tem-

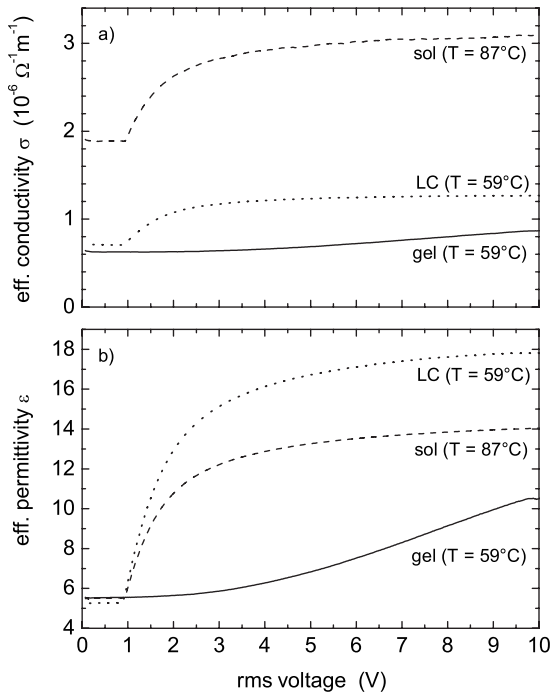

FIG. 9. Electrical detection of the Fréedericksz threshold: Effective conductivity (a) and effective permittivity (b) as functions of the driving voltage. The solid line corresponds to the gel phase and the dashed line corresponds to the sol phase. For comparison, the dotted line shows the result for the pure liquid crystal.

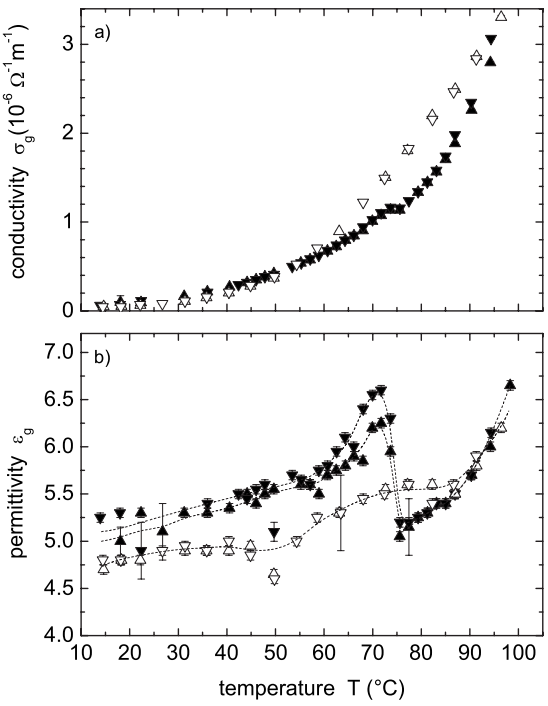

FIG. 10. Ohmic conductivity (a) and electrical permittivity (b) in the ground state as functions of the sample temperature: nematic gel with increasing (▲) and decreasing (▼) voltage; pure liquid crystal with increasing (△) and decreasing (▽) voltage. The dashed lines in diagram (b) are guides to the eye.

peratures, when the gel network has been melted, the sample again shows the typical Fréedericksz behavior [Fig. 8(c)]. Now the sample is very similar to the pure liquid crystal, since the low concentration of the melted gelator in the sol phase hardly influences the properties of the nematic liquid crystal.

In the gel phase, the decrease of the transmitted light intensity as a function of the applied voltage is still superimposed by a weak oscillation. Whether this oscillation starts with an increase or a decrease of the intensity depends on the difference of the lengths of the optical paths of the extraordinary and the ordinary beam, which in turn depends strongly on the temperature (and in principle also on the cell thickness which is not varied here). An increasing start of the oscillation leads to a seemingly higher onset voltage than a decreasing start, which makes this optical method not very well suited to determine the Fréedericksz threshold for the material in the gelified phase.

Therefore, we also consider the electrical properties of the sample, namely the effective ohmic conductivity σ and the effective electrical permittivity ϵ, as determined by Eq. (4). As shown in Fig. 9, both σ and ϵ show a sharp threshold behavior in the pure liquid crystal as well as in the sol phase, when no established gel network exists. In the gelified phase, again no sharp threshold can be detected. However, the dependence of σ and ϵ on the applied voltage is monotonous with no oscillations superimposed, thus making the electrical properties more suitable for the threshold measurements than the optical method.

C. Results

The ohmic conductivity σ_g and the electrical permittivity ϵ_g of the ground state are given by the limits of the effective conductivity σ and the effective permittivity ϵ when the voltage approaches zero. The temperature dependences of these values are shown in Fig. 10. For the conductivity and permittivity measurements, we find a characteristic kink at $T=73$ °C, which is above $T_{gs}=66$ °C revealed by the rheological measurements in Sec. III D. As observed by polarizing microscopy (see Sec. III B), there are still remains of the gelator network for $T>T_{gs}$, which explains this temperature difference.

As described in Sec. IV A, the ground-state values σ_g and ϵ_g are roughly given by $\sigma_\perp$ and $\epsilon_\perp$. In the gel phase, however, our electrical method still measures a superposition of $\sigma_\perp$ and $\sigma_\parallel$ (and $\epsilon_\perp$ and $\epsilon_\parallel$, respectively), because the gel network induces a small perturbation in the director alignment. Since E49 has a positive anisotropy of the conductivity ($\sigma_\parallel > \sigma_\perp$) as well as a positive dielectric anisotropy ($\epsilon_\parallel > \epsilon_\perp$), this perturbation leads to an increase of the measured effective values. This is verified by the observation that the permittivity ϵ of the gel phase [solid symbols in Fig. 10(b)] is systematically larger than the permittivity of the pure liquid crystal [open symbols in Fig. 10(b)] by about 0.5. We cannot observe a similar deviation between the gel phase and the pure liquid crystal for the conductivity measurement [Fig. 10(a)]. This can be explained by the high sensitivity of the conductivity σ to impurities in the material, which superimposes that effect here. When the gel network is melted at

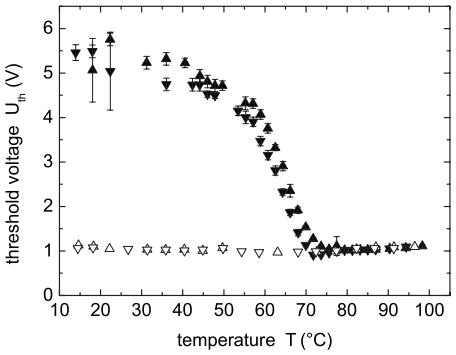

FIG. 11. Fréedericksz threshold voltage as a function of the sample temperature: nematic gel with increasing (▲) and decreasing (▼) voltage, and pure liquid crystal with increasing (△) and decreasing (▽) voltage.

the gel-sol transition, there is a decrease in both quantities σ and ϵ, as the perturbation of the director is reduced.

Due to the somewhat smaller temperature dependence of the electrical permittivity ϵ compared to the ohmic conductivity σ, we use ϵ to define a threshold criterion for the Fréedericksz transition in the following way: The voltage where ϵ has increased by $\Delta\epsilon=0.8$ above the permittivity of the ground state is set to be the threshold voltage. This is roughly 10% of the overall change in ϵ. For a comparison, we use the same change of $\Delta\epsilon=0.8$ as a threshold criterion for the pure liquid crystal sample, although in this case it is less then 10% of the overall change.

The temperature dependence of the Fréedericksz threshold voltage derived in this way is shown in Fig. 11. Here, the gel-sol transition can be clearly identified. For temperatures $T<T_{gs}$, the nematic gel shows a higher threshold voltage than the pure liquid crystal, while for temperatures $T>T_{gs}$ the thresholds are identical. For the pure liquid crystal, our threshold criterion yields a critical voltage of $U_{\mathrm{th}}^{\mathrm{LC}}=1.06$ V with no significant dependence on the temperature [39]. In the gel phase, however, there is a strong temperature dependence of the threshold voltage. At $T=15$ °C we find a threshold voltage of $U_{\mathrm{th}}^{\mathrm{gel}}\approx 5.3$ V which decreases slowly to $U_{\mathrm{th}}^{\mathrm{gel}}\approx 4.6$ V at $T=50$ °C. For higher temperatures, there is a strong decrease in the threshold voltage, reaching $U_{\mathrm{th}}^{\mathrm{sol}}=1.06$ V at $T=73$ °C. In the sol phase, the threshold voltage shows no significant temperature dependence, as is the case for the pure liquid crystal.

For temperatures below $T=73$ °C there is a systematic difference between the results for the Fréedericksz threshold of the gel (solid symbols in Fig. 11) obtained with increasing and decreasing voltage, which manifests itself also in the measurements of the electric permittivity ϵ_g in the ground state [see Fig. 10(b)]. We believe, that this is not a real hysteresis, but rather induced by an increase of the relaxation time in the gel phase. This assumption is justified by the observation, that after having waited for 3 h before the next measurement starts, the permittivity ϵ has decreased again.

V. SUMMARY AND CONCLUSION

We have prepared a nematic thermoreversible gel with the liquid crystalline mixture E49 and 0.2% of the organogelator *N*-(2-methyl-4-tetradecoylamino-phenyl)-cyclohexanecarboxamide. Characterization was performed by the falling ball method, by optical polarizing microscopy and by rheological measurements. The system exhibits a clearing range of $T_{ni}=102$ °C,…,112 °C and a gel-sol transition range of $T=58$ °C,…,73 °C, with a rheologically determined gel-sol transition temperature of $T_{gs}=66$ °C.

We applied optical and electrical methods to investigate the electric field-induced Fréedericksz effect in the material. Any hints of a qualitative change of the Fréedericksz transition have not been found. The gelator causes an increase in the Fréedericksz threshold voltage, which can be adjusted within a large range by selecting the temperature of the sample. This is a direct manifestation of the thermodynamic properties of the physical gel.

The interesting question remains, whether the Fréedericksz threshold in the gel is still characterized by a critical voltage or whether it is given by a critical field, because the director may now be anchored in the bulk rather than at the surfaces [10]. In order to answer this question, measurements using different sample thicknesses will have to be carried out, a project which we see as a natural next step in the framework of these investigations.

ACKNOWLEDGMENTS

The authors thank Dr. Nils Mohmeyer and Dr. Hans-Werner Schmidt, Makromolekulare Chemie I, Universität Bayreuth, for providing the gelator (Fig. 1). The authors thank Werner Reichstein for performing the SEM measurements (Fig. 2). The authors gratefully acknowledge the financial support of the Deutsche Forschungsgemeinschaft (DFG) Contract No. FOR608, project "Thermoreversible liquid crystalline gels under the influence of electric fields."

[1] D. R. Picout and S. B. Ross-Murphy, in *Polymer Gels and Networks*, edited by Y. Osada and A. R. Khokhlov (Marcel Dekker, New York, 2002), p. 27.
[2] R. A. M. Hikmet and H. Kemperman, Nature **392**, 476 (1998).
[3] E. M. Terentjev, M. Warner, R. B. Meyer, and J. Yamamoto, Phys. Rev. E **60**, 1872 (1999).
[4] P. A. Kossyrev, J. Qi, N. V. Priezjev, R. A. S. Pelcovits, and G. P. Crawford, Appl. Phys. Lett. **81**, 2986 (2002).
[5] D.-U. Cho, Y. Yusuf, S. Hashimoto, P. E. Cladis, H. R. Brand, H. Finkelmann, and S. Kai, J. Phys. Soc. Jpn. **75**, 083711 (2006).
[6] A. M. Menzel and H. R. Brand, J. Chem. Phys. **125**, 194704 (2006).
[7] A. M. Menzel and H. R. Brand, Phys. Rev. E **75**, 011707 (2007).
[8] D.-U. Cho, Y. Yusuf, P. E. Cladis, H. R. Brand, H. Finkelmann,

and S. Kai, Jpn. J. Appl. Phys., Part 1 **46**, 1106 (2007).
[9] A. M. Menzel, H. Pleiner, and H. R. Brand, J. Chem. Phys. **126**, 234901 (2007).
[10] C. C. Chang, L. C. Chien, and R. B. Meyer, Phys. Rev. E **56**, 595 (1997).
[11] N. Mizoshita, K. Hanabusa, and T. Kato, Displays **22**, 33 (2001).
[12] R. H. C. Janssen, J. P. Teunissen, S. J. Picken, C. W. M. Bastiaansen, D. J. Broer, T. A. Tervoort, and P. Smith, Jpn. J. Appl. Phys. **40**, 2372 (2001).
[13] J. Prigann, C. Tolksdorf, H. Skupin, R. Zentel, and F. Kremer, Macromolecules **35**, 4150 (2002).
[14] N. Mizoshita, K. Hanabusa, and T. Kato, Adv. Funct. Mater. **13**, 313 (2003).
[15] P. Cirkel, T. Kato, N. Mizoshita, H. Jagt, and K. Hanabusa, Liq. Cryst. **31**, 1649 (2004).
[16] M. D. Kempe, N. R. Scriggs, R. Verduzco, J. Lal, and J. A. Kornfield, Nat. Mater. **3**, 177 (2004).
[17] T. Kato, N. Mizoshita, M. Moriyama, and T. Kitamura, Top. Curr. Chem. **256**, 219 (2005).
[18] A. de Lózar, W. Schöpf, I. Rehberg, Ó. Lafuente, and G. Lattermann, Phys. Rev. E **71**, 051707 (2005).
[19] V. Fréedericksz and A. Repiewa, Z. Phys. **42**, 532 (1927).
[20] P. G. de Gennes and J. Prost, *The Physics of Liquid Crystals* (Clarendon, Oxford, 1993).
[21] When referring to concentrations, we use % always in the sense of weight percent.
[22] Article No. 30294, Merck KGaA, Darmstadt, Germany.
[23] F. Ortica, A. Romani, F. Blackburn, and G. Favaro, Photochem. Photobiol. Sci. **1**, 803 (2002).
[24] N. Mohmeyer and H.-W. Schmidt, Chem. Eur. J. **13**, 4499 (2007).
[25] Ó. Lafuente, Ph.D. thesis, Universität Bayreuth, 2005.
[26] I. Rehberg, B. L. Winkler, M. de la Torre Juárez, S. Rasenat, and W. Schöpf, Adv. Solid State Phys. **29**, 35 (1989).
[27] E.H.C. Co. Ltd., Tokyo, Japan.
[28] J. Brinksma, B. L. Feringa, R. M. Kellogg, R. Vreeker, and J. van Esch, Langmuir **16**, 9249 (2000).
[29] T. Kato, T. Kutsuna, K. Yabuuchi, and N. Mizoshita, Langmuir **18**, 7086 (2002).
[30] The oscillations are caused by the interference of the extraordinary and the ordinary ray of the incoming light. Since the difference in the optical path length depends strongly on the temperature, we get alternating constructive and destructive interference. The maximum just below the gelling temperature has the same origin.
[31] In the low viscous fluid state, the instrument works close to the lower limit of its specified sensitivity. Several measurements revealed, that in this case the sensitivity depends on the starting angle of the speed sensor. In order to get reliable results, it is exceedingly important to determine the starting angle with the highest sensitivity and to use this angle for all measurements.
[32] H. H. Winter and M. Mours, Adv. Polym. Sci. **134**, 165 (1997).
[33] L. Bata, A. Buka, and I. Janossy, Solid State Commun. **15**, 647 (1974).
[34] L. M. Blinov, *Electro-Optical and Magneto-Optical Properties of Liquid Crystals* (Wiley, New York, 1983).
[35] S. Chandrasekhar, *Liquid Crystals* (Cambridge University Press, Cambridge, 1994).
[36] H. Gruler, T. J. Scheffer, and G. Meier, Z. Naturforsch. A **27A**, 966 (1972).
[37] This is not shown in our results as such high voltages would destroy the samples.
[38] B. L. Winkler, H. Richter, I. Rehberg, W. Zimmermann, L. Kramer, and A. Buka, Phys. Rev. A **43**, 1940 (1991).
[39] Since $U_{\mathrm{th}}^{\mathrm{LC}}$ is obtained using our 10% criterion, this value is somewhat higher than $U_F^{\mathrm{LC}}=0.88$ V as reported in Sec. II.